



Original Paper

<http://ajol.info/index.php/ijbcs>

<http://indexmedicus.afro.who.int>

Adsorption of a basic dye Methylene Blue in aqueous solution on a bioadsorbent from agricultural waste of *Manihot esculenta* Crantz

Bernick WEMBOLOWA TSHENE, Kifline MILEBUDI KIFUANI,
Anatole KIA MAYEKO KIFUANI*, Pitchou BOKOLOMBE NGOY and
Gracien BAKAMBO EKOKO

Laboratory of Physical Organic Chemistry, Water and Environment, Department of Chemistry and Industry, Faculty of Sciences and Technology, University of Kinshasa, P.O. Box 190 Kinshasa XI, Democratic Republic of Congo.

*Corresponding author, E-mail: anatolekifuani@gmail.com; Tel: (+243) 998229987

Received: 16-05-2024

Accepted: 26-06-2024

Published: 30-06-2024

ABSTRACT

The objectives of present study were to prepare a bioadsorbent from *Manihot esculenta* Crantz peels (MEB) and to examine its effectiveness in the removal of methylene blue (MB) dye from aqueous solution by adsorption process. The adsorption was studied in a discontinuous reactor. Effects of the following parameters were studied: dose of bioadsorbent, contact time, initial concentration and pH of MB solution. The residual concentrations of MB solution were analyzed by UV-Vis spectrophotometry. The results obtained showed that the bioadsorbent MEB has a specific surface area of $265.27 \text{ m}^2 \text{ g}^{-1}$ and a maximum observed adsorption capacity (Q_{mo}) of 94.12 mg g^{-1} . The percentage of adsorption increased with the dose of biosorbent and the time due to the availability of free sites. The adsorption was better in a basic medium, because of electrostatic interactions between negatively charged MEB surface and organic ions of MB. The dose of 800 g of bioadsorbent and a pH solution of 10 were the optimal conditions of adsorption. Pseudo-first-order model was more suitable for describing the adsorption of MB on MEB, compared with pseudo-second-order model. The Langmuir model was best for describing the adsorption of MB on MEB bioadsorbent compared to the Freundlich model. The Langmuir separation parameter R_L and Freundlich parameter $1/n$, less than 1, indicate that the adsorption of MB on MEB was favorable. The bioadsorbent MEB offers a high potential for adsorption of dyes in aqueous solutions.

© 2024 International Formulae Group. All rights reserved.

Keywords: *Manihot esculenta*, Methylene Blue, Adsorption, Bioadsorbent, Isotherms, Kinetic.

INTRODUCTION

Organic dyes are among the most dangerous water pollutants. They are present in water effluents from various industries, including textile, hair, flax, wood, silk, paper and plastic. The first use of organic dyes dates back to about 4000 years ago. Nearly 15 to 20% of the dyes used for dyeing textiles are

discharged through water effluent without prior treatment (Jain et al., 2016). Organic dyes give water pestilential odors and noticeable discolorations. They inducte environmental pollution, intoxication of aquatic fauna and, through the trophic chain, the intoxication of humans who are thus contaminated by the biomagnification effect (Vanessa et al., 2017;

Alouani et al., 2018; Kifuani et al., 2018a ; Li et al., 2021 ; Jan et al., 2022).

Methylene blue (MB), a cationic thiazine dye, is widely used for dyeing cotton, wood and silk and as chemical indicator, biological stain, and drug (Sakr et al., 2015; Wei et al., 2015 ; Pathiana et al., 2017 ; Jia et al., 2018 ; Nworie et al., 2019). It is also used for medical analysis. It can cause the following conditions through contact, inhalation or ingestion: eye burns responsible for permanent injury to the eyes of humans and animals, breathing difficulties, burning sensations in the mouth, nausea, vomiting, diarrhea, gastroenteritis, perspiration and cold sweats. The removal of methylene blue and other dyes from effluents is important for environmental and human health (Song et al., 2017; Rahimian and Zarinabadi, 2020 ; Nyakairu et al., 2024).

Various methods have been developed for dyes removal classified into biological, chemical and physical methods, including a variety of techniques such as: adsorption, advanced oxidation, biosorption, chemical and electrochemical oxidation, coagulation, filtration, flocculation, microbial and fungal decolorization, photocatalysis, nanofiltration, ozonation, reverse osmosis, etc. (Maryam et al., 2013 ; Kifuani et al., 2018b ; Mekky et al., 2020 ; Basma et al., 2023 ; Miyah et al., 2017; Raiyyaan et al., 2021). Many of these techniques have proven to be expensive or responsible for the pollution induced because of the degradation products formed, sometimes more toxic than the initial dyes themselves (Ali et al, 2021). Rahimian and Zarinabadi (2020) showed that among the processes for treating water polluted by organic dyes, adsorption turns out to be the most effective. Pathiana et al. (2013) reported that adsorption on activated carbon is an effective technique for removing organic dyes from water, but the cost of activated carbon is quite high, which limits the use of activated carbon to water purification treatment.

Abas et al. (2013) reported that the demand for efficient and low-cost adsorbents

for dye removal or heavy metals in water effluent has increased. The use of materials of agricultural origin seems to be a promising approach for wastewater treatment. Various agricultural solid waste are used such as rattan sawdust, cotton stalk, hazelnut shell, oil palm shell, coffee residue, orange peel, powdered peanut hull, sugarcane bagasse, sunflower stalks, mango seed kernel, coconut coir dust, apricot stones, groundnut shells, banana pith, yellow passion fruit waste, green pea peels, mango leaves, *Hevea brasiliensis* seed coat, coir pith and Peach stones. It is reported that plant leaves contain certain constituents, e.g. polyphenols, lignin, tanins, pigments and protein, making it suitable to provide active sites for adsorption of pollutants like organic dyes or metallic elements (Laximi et al., 2010 ; Barrios et al., 2012 ; Kassale et al., 2015 ; Jain et al., 2016 ; Kumar et al., 2017 ; Pathiana et al., 2017 ; Song et al, 2017 ; Alouani et al., 2018 ; Jia et al, 2018 ; Kifuani et al., 2018a ; Ahmad et al., 2019 ; Rahimian and Zarinabadi, 2020 ; Mobalayi et al., 2021; Hatiya et al., 2022 ; Basma et al., 2023 ; Gani et al., 2023). Thus, cassava peels (*Mannihot esculanta* Crantz), a low-cost material, was used to study its adsorption performance for methylene blue, in aqueous solution. The effects of dose of adsorbent, contact time, initial concentration and pH of methylene blue solution have been studied.

MATERIALS AND METHODS

Preparation and characterization of the bioadsorbent (MEB)

Peels of *Mannihot esculenta* were collected from the city of Mbanza Ngungu, Province of Kongo Central, Democratic Republic of Congo. They were washed several times with distilled water to remove impurities from its surface, and then dried in an oven at 105 °C for 24 h (DESPATCH Oven Co, type Elect). After drying, the peelings were crushed (Industrial high speed grinder) and sieved to obtain a powder with a desired particle size ranges (< 500 µm). The bioadsorbent of

Mannihot esculenta bioadsorbent (MEB) thus obtained were stored in a desiccator at laboratory temperature (28°C), to keep it free from moisture contact and oxidation (Kifuani et al., 2018a). The bioadsorbent was characterized by the determination of Humidity, Ash, Dry matter, pH_{ZPC}.

Humidity and dry matter

Humidity (H) and dry matter (DM) were determined by loss of weight after heating 5 g of MEB in a oven. The humidity level (%H) is calculated by the following relationship (Kifuani et al., 2018a):

$$\%H = \frac{(m_1 - m_2) \cdot 100}{m_1} \quad [1]$$

Where, m_1 and m_2 , the weights of bioadsorbent before and after steaming, respectively.

The weight of the dry matter is determined after deducting the weight of water in the initial sample.

Ash content

The ash content was evaluated by determining the weight loss after calcination of 5 g of MEB in a muffle furnace (NABER, Modèle N7/H) for 8 hours. The ash content (%A) is giving by the equation below (2):

$$\%A = \frac{(m_3 - m_4) \cdot 100}{m_3} \quad [2]$$

Where, m_3 and m_4 , the weights of bioadsorbent before and after calcination, respectively.

The weight of the dry matter is determined after deducting the weight of water in the initial sample.

Determination of pH_{ZPC}

The pH at the zero point of charge (pH_{ZPC}) was obtained by the pH drift method reported by Kifuani et al. (2012) and Musah et al. (2020). For this purpose, 100 mL of 0.01 mol L⁻¹ NaCl solution were placed in different Adsorbent (LACOPE ADX). The pH of these solutions were adjusted from 3 to 12, by

addition of HCl (0.1 N) or NaOH (0.1 N) solutions, to adjust the acidic or basic solutions, respectively. 1000 mg of bioadsorbent are then added to each solution and the suspension was stirred for 72 h and centrifuged at 3000 rpm (Centrifugeuse Labofuge 200 Heraeus). The final pH was determined with a pH-Meter (Hanna Instrument). The intersection of the curve obtained by plotting the final pH as a function of the initial pH of each solution determines the pH_{ZPC}.

Determination of specific surface area

The specific surface area (S_{MB}) was evaluated by the Kifuani method, Kifuani volume variation method (KVVM), which consists of studying, at equilibrium time, the adsorption of methylene blue with a low weight of bioadsorbent (5 mg) using increasing volumes (100 mL to 1000 mL) of MB solutions (50 mg L⁻¹). The plateau obtained by plotting the adsorption capacity (q_e) as a function of the volume (V) of the MB solution corresponds to the maximum observed adsorption capacity (q_{mo} or Q_{mo}) (Kifuani et al., 2012, Kifuani, 2013 ; Kifuani et al., 2018a). The specific surface area was then calculated using the following equation (Kifuani, 2013) :

$$S_{MB} = Q_{mo} \cdot N_A \cdot s \quad [3]$$

Where, S_{MB} the specific surface area was determined using MB as adsorbate (m² g⁻¹), Q_{mo} the maximum observed adsorption capacity (mg g⁻¹), N_A the Avogadro number (6.022 10²³ mol⁻¹) and s , the area occupied by a MB molecule (175 Å²).

Adsorbate: methylene blue dye

Methylene Blue dye was used as a model of organic dye in this study, because of its flat surface known in the literature (175 Å²). His IUPAC name is 3,7- Bis (dimethylamino)phenothiazin- 5- ium chloride. It is a cationic dye heaving chemical formula C₁₆H₁₈N₃SCl, and Mw 319.852 g mol⁻¹. It was obtained from Merck and used without purification. All the reagents used in this study

were of analytical grade. The structure of MB blue is given by Figure 1.

MB solutions were prepared in pure water by dilutions from a concentrate solution of MB. The MB solutions, before and after adsorption, were analyzed using a UV-Vis spectrophotometer

(HACK Spectrophotometer, SP, model 1105) at maximum length wave, determined experimentally, by scanning in the range of 400 nm to 700 nm, for each pH studied in this paper (3-12). The residual concentration was calculated from the Beer-Lambert law, giving by equation 4 below (Kifuani, 2018a):

$$A = \epsilon.l.C \quad [4]$$

With, A being the absorbance, ϵ the molar absorption coefficient ($L \text{ mg}^{-1} \text{ cm}^{-1}$), l the thickness of the cell (1cm) and C , the concentration of the solute (mg L^{-1}).

Batch adsorption experiments

Before use, the MEB bioadsorbent was dried in an oven at 105°C for 3 h. Different weights of MEB were weighed (1 mg – 1000 mg) using an analytical balance (HEB-E 303). Adsorption was studied for different concentrations (5 mg L^{-1} - 100 mg L^{-1}) and pH (3 – 12) of MB solutions, different weights of bioadsorbent (1mg – 1000 mg) and different contact times (0 - 450 minutes). The pH of the solutions were adjusted with 0.1N of HCl or NaOH solutions for acidic or basic solutions, respectively. The adsorption tests were carried out in an adsorber (LACOPE ADS) with 100 mL of MB solution. After stirring for the required time, the suspension was centrifuged at 3000 rpm for 30 minutes and the supernatant was analyzed with a UV-Vis spectrophotometer at the appropriate wavelength, to determine the residual concentration of the MB solution. Each experiment is repeated three times to determine the absolute error.

The adsorption capacity (Q_e) and the adsorption percentage ($\%Ads$) were calculated using Eqs. (5) and (6), respectively (Mobalaji et al., 2021):

$$Q_e = \frac{(C_o - C_e)V}{m_B} \quad [5]$$

$$\% Ads = \frac{C_o - C_e}{C_o} \times 100 \quad [6]$$

With, Q_e being the apparent adsorption capacity or the equilibrium capacity of the bioadsorbent (mg g^{-1}), C_o the initial concentration of methylene blue solution (mg L^{-1}), C_e the residual or equilibrium concentration (mg L^{-1}), V the volume of the methylene blue solution (L) and $\%Ads$, the adsorption percentage.

Adsorption kinetics

The adsorption kinetics were evaluated using Lagergren pseudo-first-order and pseudo-second-order models giving by the following equations (Mekky et al., 2020):

Lagergren Pseudo-first-order model:

$$\frac{dq_t}{dt} = k_1(q_e - q_t) \quad [7]$$

$$\ln(q_e - q_t) = \ln q_e - k_1 t \quad [8]$$

Lagergren Pseudo-second-order model

$$\frac{dq_t}{dt} = k_2(q_e - q_t)^2 \quad [9]$$

$$\frac{1}{(q_e - q_t)} = \frac{1}{q_e} + k_2 t \quad [10]$$

In this study, pseudo-first-order and pseudo-second-order model equations modified by Kifuani, were used (Kifuani et al, 2012 ; Kifuani, 2013):

Kifuani Pseudo-first-order kinetic model:

$$\ln \frac{q_e}{(q_e - q_t)} = k_1 t \quad [11]$$

With, q_e being adsorption capacity at equilibrium (mg g^{-1}), q_t adsorption capacity at time t (mg g^{-1}), $q_e - q_t$ adsorption capacity of free sites, t the time (s) and k_1 , the constant rate of pseudo-first order reaction (min^{-1}).

The plot of $\ln \frac{q_e}{(q_e - q_t)}$ versus t gives a line

whose slope corresponds to k_1 , the rate constant of pseudo-first-order reaction.

Kifuni Pseudo-second-order kinetic model :

$$\frac{q_t}{q_e(q_e - q_t)} = k_2 t \quad [12]$$

Where, k_2 is the rate constant of the pseudo second order reaction ($\text{g mg}^{-1} \text{min}^{-1}$).

The plot of $\frac{q_t}{q_e(q_e - q_t)}$ versus t , give a line

whose slope corresponds to k_2 , the rate constant of the pseudo-second-order reaction.

Adsorption isotherms

The adsorption isotherms were determined for pH 3 to 12 by application of linear models of Langmuir and Freundlich, giving by the following equations (Alouani et al., 2018):

Langmuir model :

$$\frac{1}{Q_e} = \frac{1}{Q_m} + \frac{1}{Q_m K_L} \cdot \frac{1}{C_e} \quad [13]$$

Where, Q_e is the apparent adsorption capacity of the bioadsorbent (mg g^{-1}), Q_m the adsorption capacity at saturation or maximum adsorption capacity (mg g^{-1}), K_L equilibrium constant adsorption (L mg^{-1}) and C_e , equilibrium concentration.

The plot of $1/Q_e$ versus $1/C_e$ gives a line which allows to determine Q_m and K_L , from the intercept and slope, respectively.

The Langmuir separation parameter (R_L) was calculated by the following equation (Alouani et al., 2018) :

$$R_L = \frac{1}{1 + K_L C_o} \quad [14]$$

K_L is the Langmuir constant (L mg^{-1}) and C_o the initial dye concentration.

Freundlich model :

$$\text{Log } Q_e = \text{log } K_F + \frac{1}{n} \text{log } C_e \quad [15]$$

Where, Q_e the adsorption capacity at equilibrium (mg g^{-1}), K_F the adsorption constant (Freundlich constant), C_e the concentration of the adsorbate at equilibrium (mg L^{-1}) and n , the Freundlich constant, characterizing the affinity of solute for the adsorbent (affinity parameter).

The plot of $\text{log } Q_e$ versus $\text{log } C_e$ gives a line which allows to determine K_F and $1/n$ from the intercept and slope, respectively.

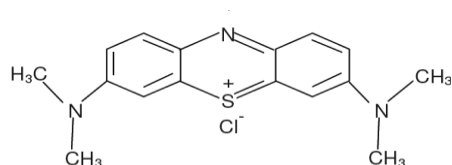


Figure 1: Structure of Methylene Blue.

RESULTS

Characteristics of the bioadsorbent

Table 1 present the physicochemical characteristics of MEB bioadsorbent. The bioadsorbent has a specific surface area of $265.27 \text{ m}^2 \text{ g}^{-1}$ and a maximum observed adsorption capacity (Q_{m0}) of 94.12 mg/g . The pH_{ZPC} of the adsorbent is 5.24.

Effect of bioadsorbent dosage

In order to estimate the optimal weight necessary to eliminate methylene blue, 100 mL of the methylene blue solution, with a concentration of 50 mg L^{-1} , were brought into contact with different weights of bioadsorbent at the self-equilibrium pH (6.64). The results obtained are shown in Table 2 and Figures 2 and 3. Figure 2 gives a plot of maximum adsorption capacity (Q_m) versus the dose of adsorbent. The results reported in Figure 3 show that when the weight of the bioadsorbent increases, from 1 to 1000 mg, the maximum percentage adsorption ($\%_{mAds}$) also increases from 10.94% to 76.38%. The optimal adsorption weight was evaluated at 800 mg, with a maximum adsorption percentage of 76,5%, after 270 min. After this weight, the adsorption tends towards constancy.

Effect of contact time

The adsorption tests were carried out from 0 to 450 minutes, first with a methylene blue solution 50 mg L^{-1} for different weights of adsorbent, after, with different initial concentrations and pH of BM solutions using

800 g of MEB. The results obtained are given by Table 2, and Figures 4 to 9.

Effect of initial Methylene blue concentration

The effect of the initial concentration on adsorption was studied at self-equilibrium pH 6.64. The results obtained are presented in Figures 10 and 11. Figure 10 shows an increase in the maximum adsorption capacity, when the initial concentration of methylene blue increases. The results presented in Figure 11 show a decrease in the adsorption percentage with the increase of initial concentration. The maximum percentage adsorption ($%_mAds$) decreases from 87.06% to 74.24% when the MB concentration increase from 10 mg/L to 100 mg/L. After the initial concentration of 50 mg L⁻¹, the adsorption percentage tends to a constant value (74,31%).

Effect of pH

The effect of MB pH solution on the adsorption is given by Table 3, Figures 12 and 13. These results report that the maximum adsorption capacity and the maximum adsorption percentage increase with the pH of MB solution and tend to a constant value after pH 10, which is than the optimum pH, with the maximum adsorption percentage of 78.74% after 270 minutes. The pH of 10 was chosen as

the optimum pH for adsorption of MB on MEB bioadsorbent with 78.74% of MB removal.

Modeling of adsorption kinetics

Only the kinetic results obtained for the adsorption of BM on the MEB bioadsorbent with the optimal weight (800 mg) were modeled using the kinetic equations of the pseudo-first-order and pseudo-second-order surface reaction. Table 4 shows the kinetic parameters for the adsorption at different pH. The k_1 constants range from 0.090 min⁻¹ to 0.0174 min⁻¹, while the k_2 values range from 0.0056 g mg⁻¹ min⁻¹ to 0.0197 g mg⁻¹ min⁻¹.

Modeling of adsorption isotherms

The adsorption isotherms were obtained at different pH (3-12) using 800 mg of bioadsorbent, 100 mL of MB solution 50 mg L⁻¹. The suspensions were stirred for 300 minutes, time being in the equilibrium range. The modeling of the isotherms was done with the Langmuir and Freundlich isotherm models. By linearization, the following parameters were determined: Q_m , K_L , R_L for Langmuir ; K_F and $1/n$ for Freundlich. Table 5 presents the Langmuir and Freundlich parameters determined.

Table 1: Characteristics of MEB bioadsorbent.

Parameters	Values
Particle seize (mm)	≤ 0,50
Humidity (%)	2,95
Dry matter (%)	97,05
Ash (%)	4,32
pH _{zpc}	5,24
Q_{mo} (mg g ⁻¹)	94,12
Specific area, S_{MB} (m ² g ⁻¹)	265,27

Table 2: Equilibrium concentration (C_e), maximum adsorption capacity (Q_m), maximum percentage of adsorption ($\%mAds$), equilibrium time (t_e) at different weights of bioadsorbent (m_{BA}).

m_{BA} (mg)	C_e (mg L ⁻¹)	Q_m (mg g ⁻¹)	$\%mAds$	t_e (min)
1	44,5	547,0	10,94	330
5	41,7	165,9	16,59	300
50	37,4	25,2	25,20	300
100	28,8	21,2	42,47	270
200	15,2	17,4	69,53	270
400	13,8	9,0	72,35	270
600	12,6	6,2	74,71	270
800	11,8	4,8	76,35	270
1000	10,4	4,0	76,38	270

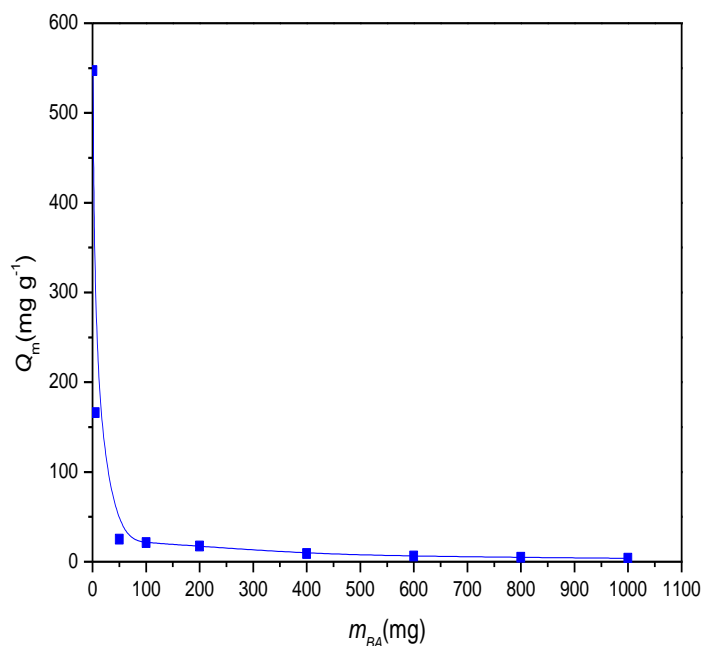


Figure 2: The maximum adsorption capacity (Q_m) vs dose of bioadsorbent (mg) (C_0 : 50 mg L⁻¹ ; pH : 6.64 ; V : 100 mL ; T : 28,0°C ; λ_{max} : 662 nm).

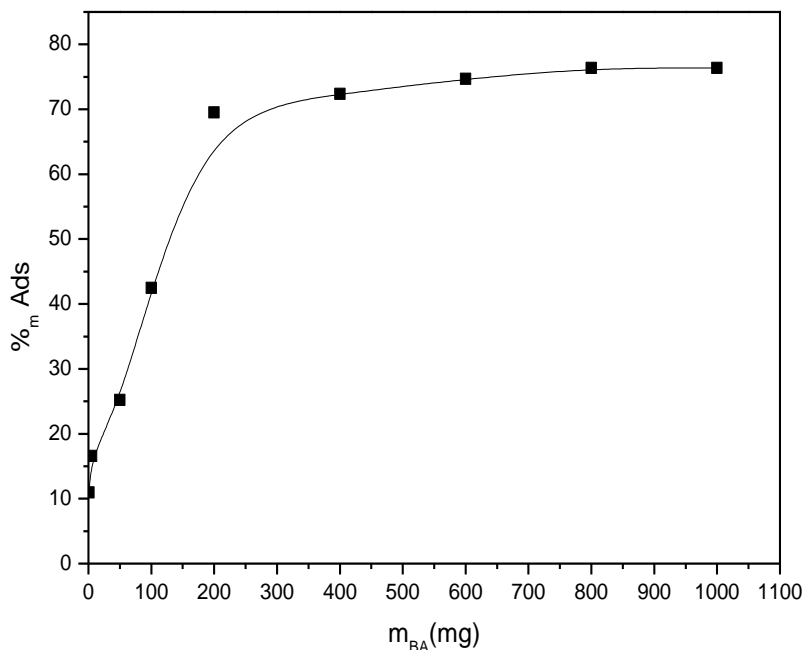


Figure 3: The maximum percentage of adsorption (%_mAds) vs. dose of bioadsorbent (mg) (C_0 : 50 mg L⁻¹ ; pH : 6.64 ; V : 100 mL ; T : 28,0°C ; λ_{max} : 662 nm).

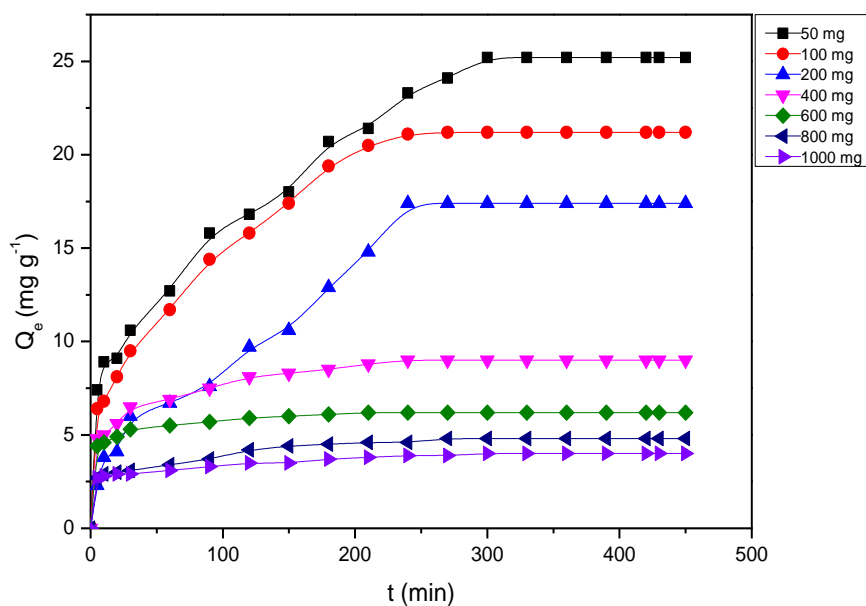


Figure 4: Effect of contact time on adsorption capacity (Q_e) of MEB at different dose of adsorbent (C_0 : 50 mg L⁻¹ ; pH : 6.64 ; V : 100 mL ; T : 28,0°C ; λ_{max} : 662 nm).

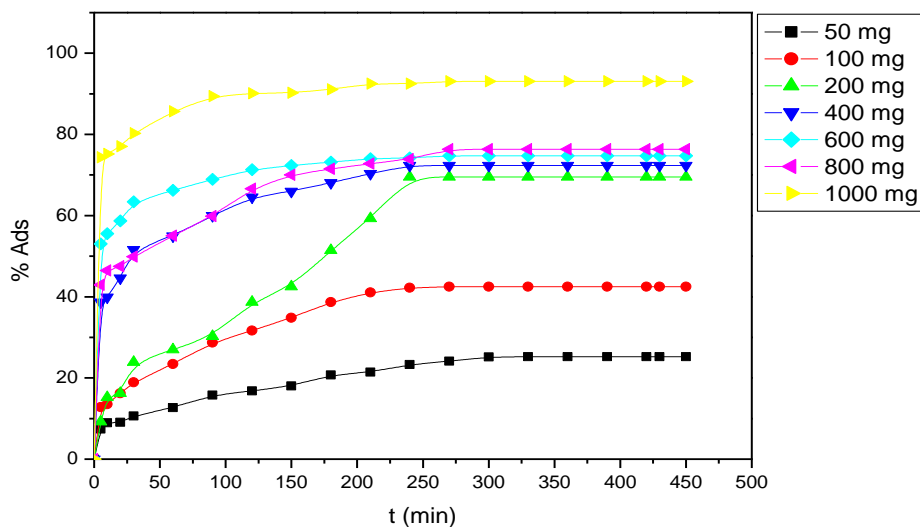


Figure 5: Effect of contact time on the percentage of MB adsorption on MEB at different dose of adsorbent (C_0 : 50 mg L⁻¹; pH: 6.64; V : 100 mL; T : 28,0 °C; λ_{max} : 662 nm).

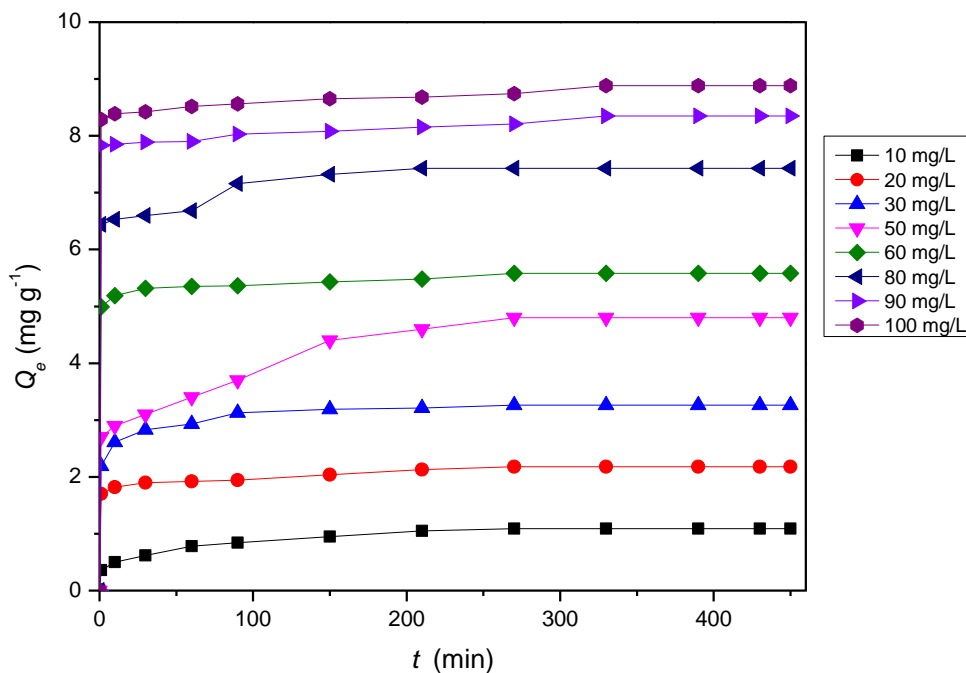


Figure 6: Effect of contact time at different initial concentrations (V : 100 mL; pH 6.64; m_{BA} : 800 mg; T : 28,0°C).

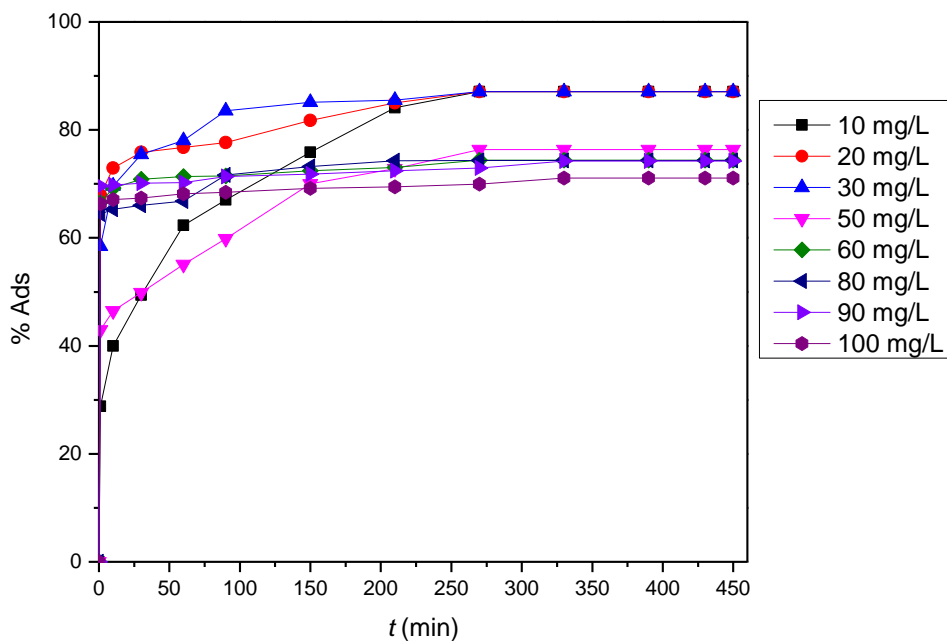


Figure 7: Effect of contact time on the percentage of MB adsorption on BME at different initial concentrations (V : 100 mL ; pH 6.64 ; m_{BA} : 800 mg ; T : 28,0°C).

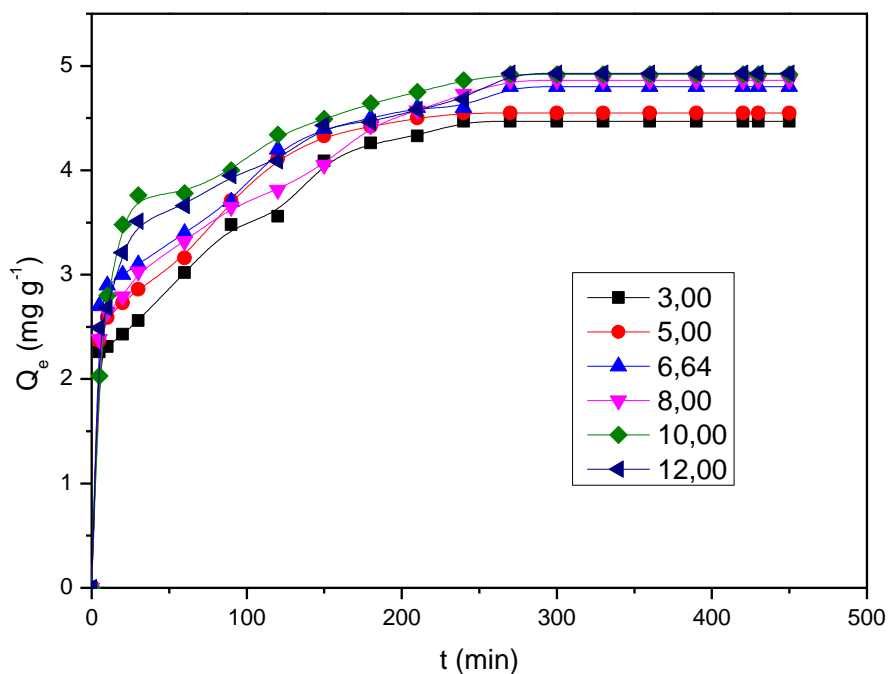


Figure 8: Effect of contact time on the adsorption capacity of BME at different pH (C_0 : 50 mg L⁻¹ ; V : 100 mL ; m_{BA} : 800 mg ; T : 28,0°C).

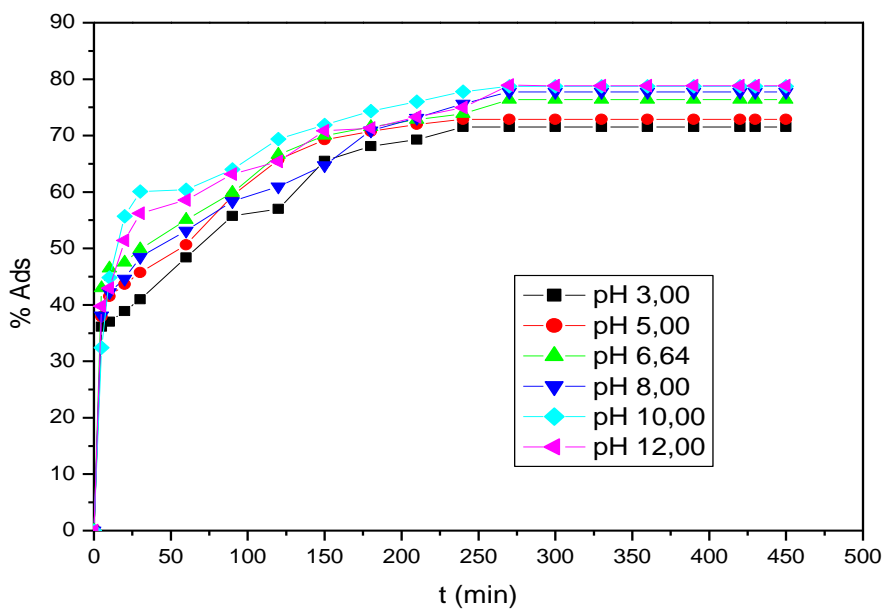
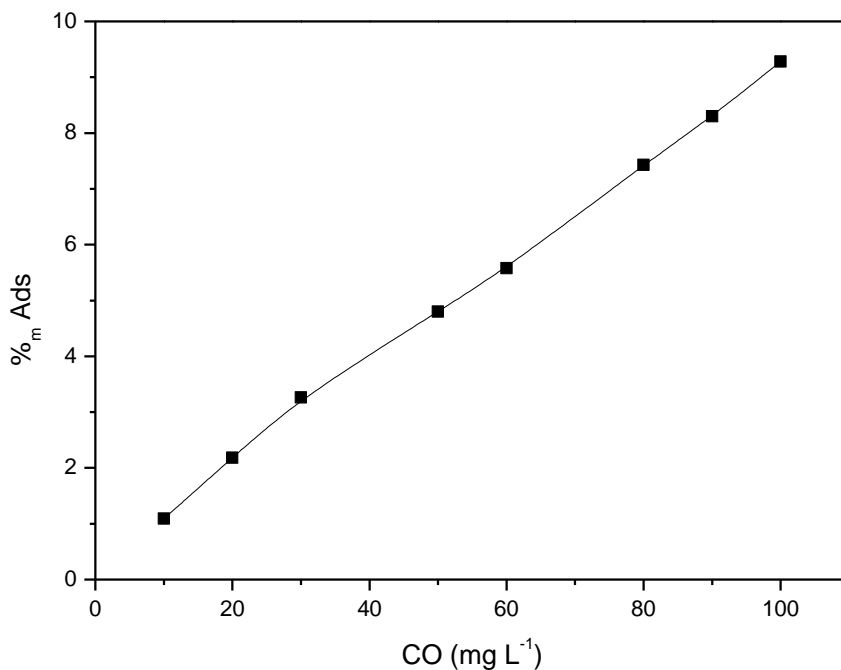


Figure 9: Effect of contact time on the percentage of MB adsorption on BME at different pH (C_0 : 50 mg L⁻¹ ; V : 100 mL ; m_{BA} : 800 mg ; T : 28,0°C).



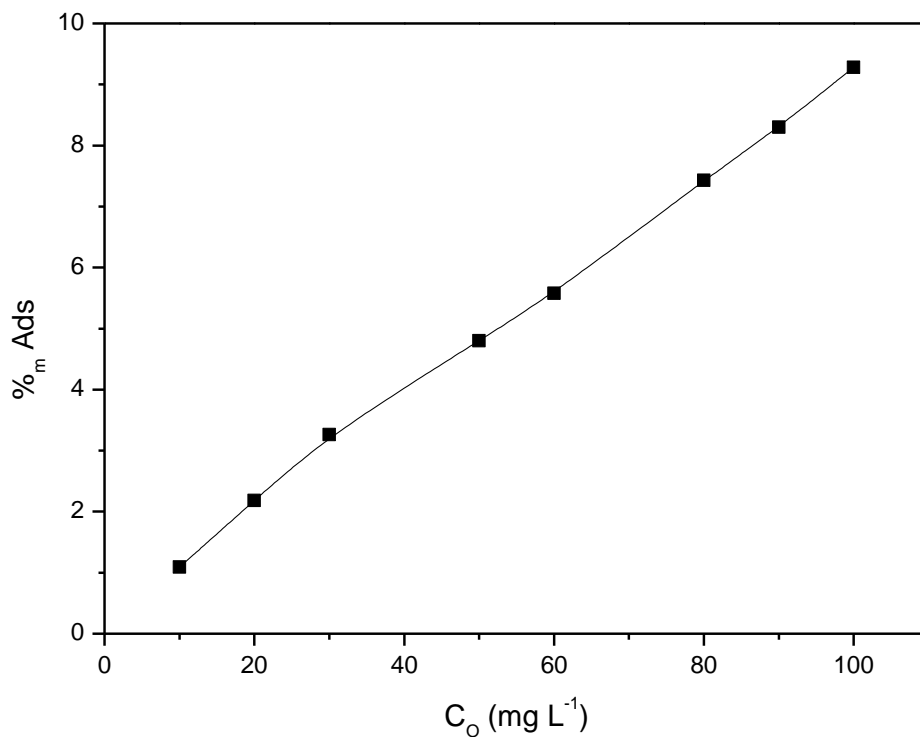
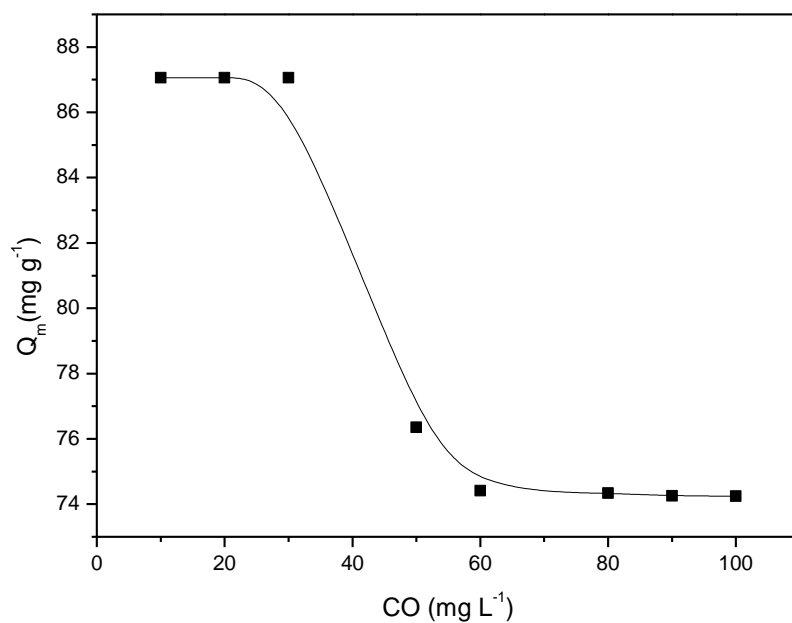


Figure 10: Effect of initial concentration of MB on the maximum adsorption capacity of MEB (V : 100 mL; pH: 6.64; m_{BA} : 800 mg ; T : 28,0°C).



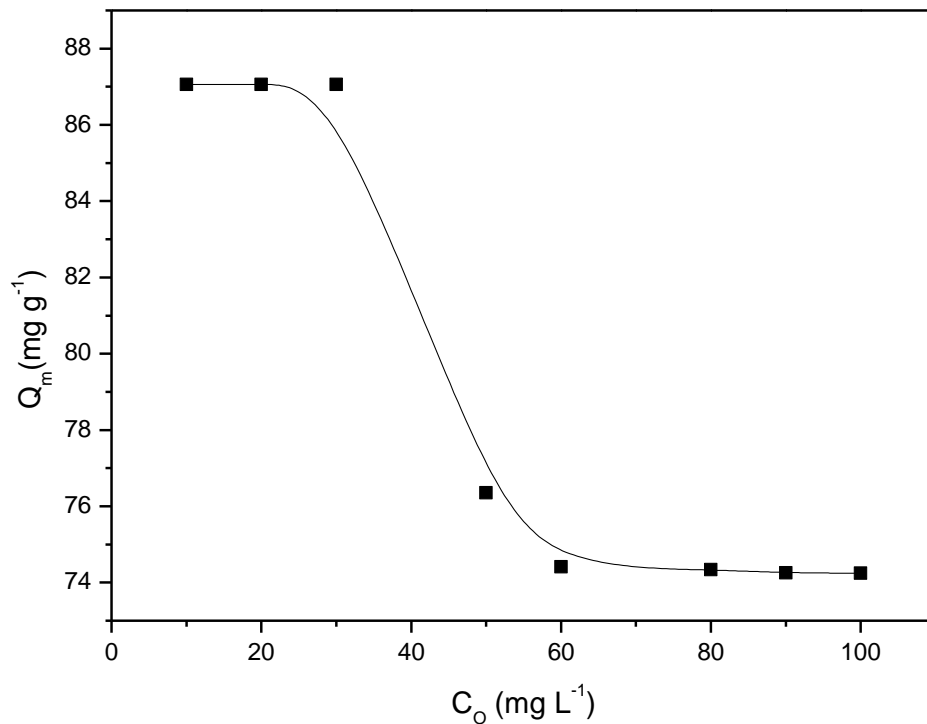


Figure 11 : Effect of initial concentration of MB on the maximum adsorption percentage of MEB (V : 100 mL ; pH : 6.64 ; m_{BA} : 800 mg ; T : 28,0°C).

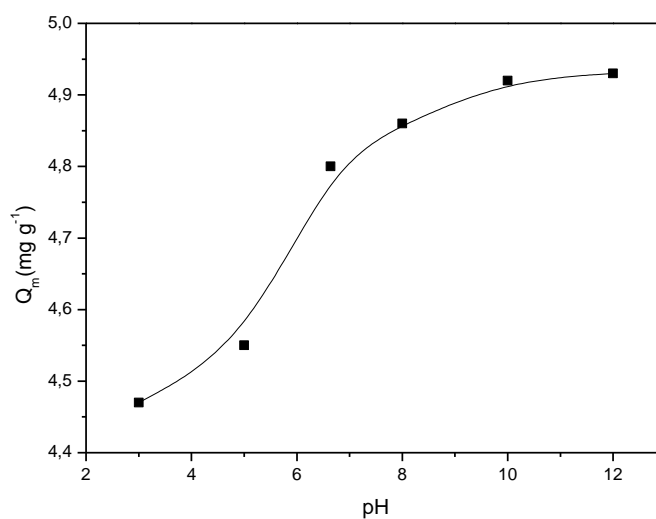


Figure 12: Effect of pH on the maximum adsorption capacity of BME (V : 100 mL ; m_{BA} : 800 mg ; T : 28,0°C).

Tableau 3: Maximum adsorption capacity (Q_m), maximum percentage adsorption ($\%_m\text{Ads}$), and equilibrium time (t_e) at different pH.

pH	Q_m (mg g ⁻¹)	$\%_m\text{Ads}$	t_e (min)
3,00	4,5	71,50	240
5,00	4,6	72,88	240
6,64	4,8	76,35	270
8,00	4,9	77,75	270
10,00	4,9	78,74	270
12,00	4,9	78,82	270

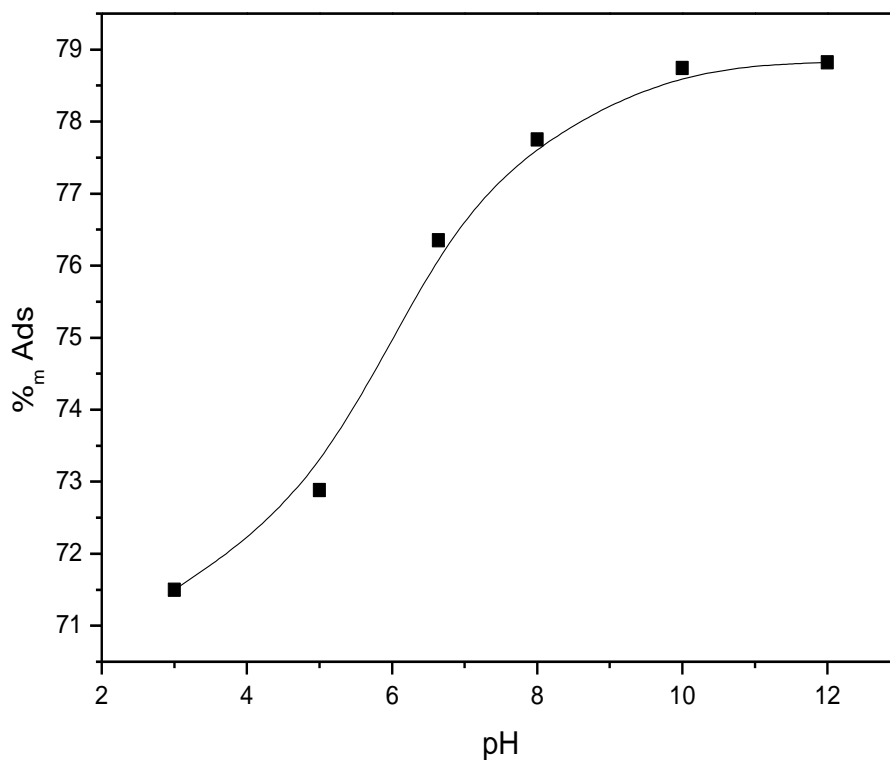


Figure 13: Effect of pH on the maximum adsorption percentage of MEB (V : 100 mL ; m_{BA} : 800 mg; T : 28,0°C).

Table 4: Pseudo-first- order and pseudo-second-order parameters for the adsorption of MB onto MEB at different pH.

pH	Pseudo-first- order parameters		Pseudo-second-order parameters	
	k_1 (min ⁻¹)	R ²	k_2 (g mg ⁻¹ min ⁻¹)	R ²
3	0,0133	0,9581	0,0061	0,9694
5	0,0174	0,9679	0,0138	0,8675
6,64	0,0109	0,9806	0,0197	0,9175
8	0,0094	0,9597	0,0056	0,9604
10	0,0133	0,947	0,0153	0,9081
12	0,009	0,9821	0,0109	0,9496

Table 5: Langmuir and Freundlich parameters for the adsorption of MB onto MEB at différénts pH.

pH	Langmuir parameters				Freundlich parameters		
	Q_m (mg/g)	K_L (L mg ⁻¹)	R_L	R ²	K_f *	1/n	R ²
3.00	4,5	0.0744	0,2118	0,9180	0.0062	1.6813	0,7572
5.00	4,6	0.0455	0,3053	0,8242	2.6255	0.1406	0,7416
6,64	4,8	0.0548	0,2675	0,9665	0.8089	0.4552	0,8542
8.00	4,9	0.0596	0,2513	0,8521	2.5318	0.1668	0,7384
10.00	4,9	0.0412	0,3266	0,9039	3.3394	0.0991	0,9131
12.00	4,9	0.0521	0,2772	0,9582	3.0290	0.1245	0,8917

k_f * unit : (mg g⁻¹) (mg L⁻¹)^{-1/n})

DISCUSSION

The maximum observed adsorption capacity (Q_{mo}) determined for the MEB is significantly better compared to those reported by Rahimian and Zarinabadi (2020) with 40.0 mg g⁻¹ for the leaves of pine trees bioadsorbent. The pH_{ZPC} of MEB shows that the surface of the bioadsorbent is neutral at pH 5.24. The surface of the bioadsorbent is thus positive at pH <5.24 and negative at pH >5,24.

The decrease of the maximum adsorption capacity of the bioadsorbent with increasing of weight of bioadsorbent (Figure 2) is explained by the weight effect of the bioadsorbent, characterized by an agglomeration of the bioadsorbent particles. Certain particles do not participate in adsorption when the weight of the bioadsorbent increases, although they are taken into account when expressing the adsorption capacity (Jain

et al., 2016; Kifuani et al., 2018a). The increase of the maximum adsorption percentage of the bioadsorbent with increasing of weight of bioadsorbent (Figure 3) is explained by the fact that the increase in the weight of the adsorbent increases the availability of free sites, which are gradually saturated (Kifuani, 2018a ; Song et al., 2017).

These results of Figures 4 to 9 show that the apparent adsorption capacity (Q_e) and the apparent adsorption percentage ($\%Ads$) increase with the increase of contact time MB-MEB, until a maximum value which remains constant despite the increase in time. These maximum values correspond to the apparent maximum adsorption capacity (Q_m) or the apparent maximum adsorption percentage ($\%_mAds$). These increase of adsorption capacity or adsorption percentage are explained by the availability of free sites, which are gradually saturated (Wei et al., 2015).

From the results of Figures 10 and 11, it appears that the quantity of methylene blue retained by the bioadsorbent is higher, and the adsorption mechanism is more efficient, with the increase in the initial dye concentration. The decrease of the maximum percentage adsorption when the MB concentration increase is due to the agglomeration of the solute particles (methylene blue) with the increase of initial concentration. Musah et al. (2020) also reported the same observations on the decrease in the adsorption percentage with the concentration of the solution for the adsorption of methylene blue on a bioadsorbent from *Platanus orientalis* leaf powder.

The increase of the maximum adsorption capacity and the maximum adsorption percentage with the pH of MB solution can be explained as follows : since the pH_{ZPC} of MEB is 5.4, the surface of the bioadsorbent is neutral at this pH, which reduce the attractive interactions with the organic cation ions of MB if $pH < 5.4$, the pH_{ZPC} . The surface of the bioadsorbent is negative at $pH > 5.4$, than there are strong attractive interactions with negative charges of the bioadsorbent surface and the organic cation ions of MB. Then we observe an increasing in

the adsorption capacity and adsorption percentage in basic medium compared to acidic media.

The average of the overall linear correlation coefficients (R^2_g) of the pseudo-first-order reaction model (0.9659) is higher than that of the pseudo-second-order reaction model (0.9287), indicating that the kinetic model of the pseudo-first-order reaction is better suited to describe the adsorption of methylene blue onto the bioadsorbent than the pseudo-second-order reaction. The correlation with the pseudo-first-order model indicates that the adsorption is governed by the surface reaction, characterized by the attachment of methylene blue molecules to the surface of the MEB bioadsorbent. This correlation, less than 1, does not exclude other adsorption mechanisms. Similar kinetic results have been reported in the literature (Musah et al., 2020).

The averages of the overall correlation coefficients (R^2_g) of the Langmuir model (0.9038) and the Freundlich model (0.8160) obtained (Table 5) indicate that the Langmuir model is best for describing the adsorption of MB on MEB bioadsorbent compared to the Freundlich model, indicating monolayer adsorption of BM onto the bioadsorbent. The correlation with the Freundlich model indicates, however, that additional layers are formed at high MB concentrations (Kifuani, 2013). Similar results have been reported in the literature (Ahmad et al., 2019 ; Basma et al., 2023 ; Gani et al., 2023). The K_L , equilibrium parameter or separation parameter, indicates the affinity of the bioadsorbent towards methylene blue, which can be favorable ($0 < R_L < 1$), irreversible ($R_L = 0$), linear ($R_L = 1$) or unfavorable ($R_L > 1$) (Maryam et al., 2013 ; Kumar et al., 2017). The R_L values obtained < 1 , for all pH studied, indicate that the adsorption of MB on the MEB bioadsorbent is favorable (Table 5). The K_F values represent the adsorbent power of the bioadsorbent, when the concentration (C_0) of BM is unitary. The Freundlich parameter $1/n$ indicate the adsorption intensity or adsorption interaction strength. It is reported that the adsorption can be favorable ($1/n < 1$), linear ($1/n = 1$), physical and unfavorable ($1/n > 1$) (Pathiana, 2017).

Values of $1/n$ obtained in this study are less than 1 indicate high affinity between MB and MEB surface, and thus the adsorption is favorable.

Conclusion

In this work, the adsorption of a basic dye, Methylene Blue, in aqueous solution, on a bioadsorbent from agricultural waste of *Manihot esculenta* Crantz was studied. The adsorption tests were carried out in an adsorber (LACOPE ADS) with MB solution. After stirring for the required time, the suspension was centrifuged and the supernatant was analyzed with a UV-Vis spectrophotometer, to determine the residual concentration of the MB solution. Various adsorption parameters were studied including the weight of the bioadsorbent, the bioadsorbent-BM contact time, the initial concentration and pH of MB solutions. The results obtained in this research showed that the bioadsorbent MEB has a specific surface area of $265.27 \text{ m}^2 \text{ g}^{-1}$ and a maximum observed adsorption capacity (Q_{mo}) of 94.12 mg g^{-1} . The optimal adsorption weight was evaluated at 800 mg, with a maximum adsorption percentage of 76,35%, after 270 minutes. The optimum pH was evaluated to be 10, with 78.74% after 270 minutes. The kinetic model of the pseudo-first-order reaction is better suited to describe the adsorption of methylene blue onto MEB bioadsorbent than the pseudo-second-order reaction. The Langmuir model is best for describing the adsorption of MB on MEB bioadsorbent compared to the Freundlich model. The bioadsorbent MEB has a high specific surface area and a high maximum observed adsorption capacity and thus offers a high potential for adsorption of dyes in aqueous solutions and might be used as an adsorbent for wastewater treatment.

COMPETING INTERESTS

The authors declare that they have no competing interests.

AUTHORS' CONTRIBUTIONS

BWT, KMK and AKMK are the main investigators of this study and have

participated in all the stages of the research. GBE and PBN have contributed to data processing and discussion of results.

ACKNOWLEDGEMENTS

The authors of the manuscript gratefully acknowledge the anonymous reviewers for their valuable comments on our manuscript.

REFERENCES

- Abas SN, Ismail MHS, Kamal ML, Izhar S. 2013. Adsorption process of heavy metals by low-cost adsorbent: A review. *World Appl. Sci. J.*, **28**(11): 1518-1530. DOI: 10.5829/idosi.wasj.2013.28.11.1874
- Ahmad NL, Zakariyya UZ, Usman A, Zaharaddeen NG. 2019. Rice husk as biosorbent for the adsorption of methylene blue. *Science World Journal*, **14**(2): 66-70. <https://www.scienceworldjournal.org>
- Ali K, Javaid UJ, Ali Z, Zaghum MJ. 2021. Biomass-derived adsorbents for dye and heavy metal removal from wastewater. *Adsorption Science and Technology*, **2021**: 1-14. DOI: <https://doi.org/10.1155/2021/9357509>
- Alouani MEL, Alehyen S, Achouri MEL, Taibi M. 2018. Removal of cationic dye methylene blue from aqueous solution by adsorption on fly ash-based geopolymer. *J. Mater. Envir. Sci.*, **9**(1): 32-46. DOI: <https://dx.doi.org/10.26872/jmes.2018.9.1.5>
- Barrios M, Martin M, Martin A. 2012. Treatment of pollutants in wastewater: Adsorption of methylene blue onto olive-based activated carbon. *Journal of Industrial and Engineering Chemistry*, **18**: 780-784.
- Basma G. Alhogbi GS. Al B. 2023. An investigation of a natural biosorbent for removing methylene blue dye from aqueous solution. *Molecules*, **28**(6): 2785. DOI: <https://doi.org/10.3390/molecules28062785>
- Gani P, Puji L. 2023. Comparison of two biosorbent beads for methylene blue discoloration in water. *J. Ecol. Eng.*,

- 24(8): 137-145. DOI: <https://doi.org/10.12911/22998993/166319>
- Hatiya NA, Reshad AS, Negie ZW. 2022. Chemical modification of Neem (*Azadirachta indica*) biomass as bioadsorbent for removal of Pb²⁺ ion from aqueous wastewater. *Adsorption Science and Technology*, **2022** : 1-18. DOI: <https://doi.org/10.1155/2022/7813513>
- Hatiya NA, Reshad AS, Negie ZW. 2022. Chemical modification of Neem (*Azadirachta indica*) biomass as bioadsorbent for removal of Pb²⁺ ion from aqueous wastewater. *Adsorption Science and Technology*, **2022** : 1-18. DOI: <https://doi.org/10.1155/2022/7813513>
- Jain N, Dwivedi, Waskle A. 2016. Adsorption of methylene blue dye from industrial effluents using coal fly ash. *IJAERS*, **3(4)** : 9-16. www.ijaers.com
- Jan SU, Ahmad Y, Ali M, Hussain Z, Melhi S. 2022. Adsorptive removal of methylene blue from aqueous solution using sawdust. *Medicom Pharmaceutical Sciences*, **2** (1) : 8-16.
- Jia P, Tan H, Liu K, Gao W. 2018. Removal of methylene blue from aqueous solution by bone char. *Appl. Sci.*, **1903** :1-11. DOI : 10.3390/app8101903
- Kassale A, Berouni K, Bazzouai M, Albourine A. 2015. Kinetics and modeling of the adsorption of methylene blue by the grafted cotton. *J. Chem. Bio. Phy. Sci.*, **5(2)**: 1205-1216. <http://www.jcbpsc.org>
- Kifuani AKM, Noki PV, Ndelo JDP, Mukana WM, Ekoko GB, Ilinga BL, Mukinayi JM. 2012. Adsorption de la quinine bichlorhydrate sur charbon actif peu coûteux à base de la bagasse de canne à sucre imprégnée de l'acide phosphorique. *Int. J. Biol. Chem. Sci.*, **6(3)**: 1337-1359. DOI: <https://dx.doi.org/10.4314/ijbcs.v6i3.36>
- Kifuani AKM. 2013. Adsorption des composés organiques aromatiques en solution aqueuse sur charbon actif à base des déchets agroindustriels. Thèse de doctorat, Université de Kinshasa
- Kifuani KM, Kifuani AKM, Ilinga BL, Ngoy PB, Monama TO, Ekoko GB, Mbala BM, Muswema JL. 2018a. Adsorption d'un colorant basique Bleu de Methylene en solution aqueuse sur un bioadsorbant issu de déchets agricoles de *Cucumeropsis mannii* Naudin. *Int. J. Biol. Chem. Sci.*, **12(1)**: 558-575. DOI : <https://dx.doi.org/10.4314/ijbcs.v12i1.43>
- Kifuani KM, Kifuani AKM, Ilinga BL, Ngoy PB, Monama TO, Ekoko GB, Muswema JL. 2018b. Kinetics and thermodynamic studies adsorption of Methylene Bleu in aqueous solution on a bioadsorbent from *Cucumeropsis mannii* Naudin waste seeds. *Int. J. Biol. Chem. Sci.*, **12(5)**: 2412-2423. DOI: <https://dx.doi.org/10.4314/ijbcs.v12i5.38>
- Kumar PS, Sivaprakash S, Jayakumar. 2017. Removal of Methylene Blue dye from aqueous solutions using Lagerstroemia indica seed (LIS) activated carbon. *Inter. J. Mater. Sc.*, **12(1)**: 107-116. <http://www.ripublication.com>
- Laximi G.S, Ahmazzaman MD. 2010. Adsorption technique for the removal of phenolic compounds from wastewater using low-cost natural adsorbents. *Assam Univ. J. Sci. Techn.*, **5(2)**: 156-166.
- Le PT, Bui HT, Le TH, Nguyen TH, Pham LA, Nguyen HN, Nguyen QS, Nguyen TP, Bich NT, Duong TT, Herrmann M, Ouillon, Le TPQ. 2021. Preparation and characterization of biochar derived from agricultural by-products for dye removal. *Adsorption Science and Technology*, **2021** : 1-21. DOI: <https://doi.org/10.1155/2021/9161904>
- Maryam K, Nahid G, Babak M, Mohsen R. 2013. Removal of Methylene Blue from wastewater by adsorption onto ZnCl₂ activated Corn Husk carbon : Equilibrium Studies. *Journal of Chemistry*, **2013** : 1-6. DOI : <http://dx.doi.org/10.1155/2013/383985>
- Mekky AEM, El-Masry MM, Khalifa RE, Omer AM, Tamer TM, Khan ZA, Gouda M, Mohy Eldin MS. 2020. Removal of

- methylene blue dye from synthetic aqueous solutions using dimethylglyoxime modified amberlite IRA-420: kinetic, equilibrium and thermodynamic studies. *Desalination and Water Treatment*, **181**: 399-411. DOI: 10.5004/dwt.2020.25097
- Miyah Y, Lahrichi A, Idrissi M, Anis Kh, Kachkoul R, Idrissi N, Lairini S, Nenov V, Zerrouq F. 2017. Cristal violet in aqueous solution by the local clay. *J. Mater. Environ. Sci.*, **8**(10): 3570-3582. <http://www.jmaterenironsci.com>
- Mobalaji MJ, Olatunde SD, Joshua NE. 2021. Sequestration of hazardous dyes from aqueous solution using raw and modified agricultural waste. *Adsorption Science and Technology*, **2021**: 1-21. DOI: <https://doi.org/10.1155/2021/6297451>
- Musah BM, Peng L, Xu Y. 2020. Adsorption of methylene blue using chemically enhanced Platanus orientalis leaf powder: kinetics and mechanisms. *Nat. Env. Poll. Tech.*, **19**(1): 29-40. www.neptjournal.com
- Nyakairu GWA, Kapanga PM, Ntale M, Lusamba SN, Tshimanga RM, Ammari A, Shehu Z. 2024. Synthesis, characterization and application of Zeolite/Bi₂O₃ nanocomposite in removal of Rhodamine B dye from wastewater. *Cleaner Water*, **1**: 100004. DOI: <https://dx.doi.org/10.1016/j.clwat.2024.100004>
- Pathania D, Sharma S, Singh P. 2017. Removal of methylene blue by adsorption onto activated carbon developed from *Ficus carica* bast. *Arabian Journal of Chemistry*, **10**: S1445-S1451. DOI: <https://dx.doi.org/10.1016/j.arabjc.2013.04.021>
- Rahimian R, Zarinabadi S. 2020. A review of studies on the removal of methylene blue dye from industrial wastewater using activated carbon adsorbents made from Almond Bark. *Prog. Biochem. Res.*, **3**(3): 251-268. DOI: 10.33945/PCBR.2020.3.8
- Raiyyaan GD, Khalith M SB, Sheriff AM, Arunachalam KDA. 2021. Bio-adsorption of methylene blue dye using chitosan-extracted from Fenneropenaeus indicus shrimp shell waste. *J. Aquac. Mar. Biol.*, **10**(4): 146-150. <https://medcraveonline.com>
- Sakr F, Sennaoui A, Elouardi M, Tamimi M, Assabbane A. 2015. Study of the adsorption of methylene blue on a biomaterial based on Cactus. *J. Mater. Environ. Sci.*, **6**(2): 397-406.
- Song C, Libo Z, Hongying X, Jinhui P, Jianhua S, Chunyang L, Xin J, Qi Z. 2017. Adsorption behavior of methylene blue onto waste-derived adsorbent and exhaust gases recycling. *Royal Society of Chemistry*, **7**: 27331-27341. DOI: 10.1039/C7RA01482A (Paper) RSC Adv.
- Song C, Libo Z, Hongying X, Jinhui P, Jianhua S, Chunyang L, Xin J, Qi Z. 2017. Adsorption behavior of methylene blue onto waste-derived adsorbent and exhaust gases recycling. *Royal Society of Chemistry*, **7**: 27331-27341. DOI: 10.1039/C7RA01482A (Paper) RSC Adv.
- Vanessa Peings V, Andrin A, Le Behec M, Lacombe S, Frayret J, Pigot T. 2017. Couplage photocatalytique-oxydation par le ferrate-VI pour le traitement du colorant Rhodamine 6G. *Revue des Sciences de l'Eau*, **30**(1): 35-39. DOI: <https://dx.doi.org/10.7202/104006Lar>
- Wei W, Yang L, Zhong WH, LI SY, Cui J, Wei ZG. 2015. Fast removal of methylene blue from aqueous solution by adsorption onto poorly crystalline hydroxyapatite nanoparticles. *Digest Jour. Nanomat. Biores.*, **10** (4): 1343-1363.